3D FE analysis of anchor bolts with large embedment depths

J. Ožbolt, R. Eligehausen & G. Periškić
Institute of Construction Materials, University of Stuttgart, Stuttgart, Germany
U. Mayer
Nolasoft - design office, Stuttgart, Germany

ABSTRACT: In the present paper the results of a finite element study of single headed stud anchors loaded in tension (concrete cone failure) and shear (concrete edge failure) are discussed. Anchors with extremely large embedment depths (up to 1500 mm) for which little experimental data is available are investigated. Many such anchors are used in engineering practice, therefore, the aim of the study was to investigate their safety. The numerical analysis is performed using a three-dimensional finite element code based on the microplane model. Calculated concrete cone capacity for large anchors with small heads show good agreement with the current design formula for anchors, which is based on LEFM. For anchors with larger heads, the ultimate resistance is higher than predicted by the design code formula and the size effect on the ultimate load is less pronounced. To account for the effect of the size of the headed stud, an additional influencing factor is proposed. Numerical results for large anchors loaded in shear agree well with the test results. The results indicate that the current design formula is unsafe for large anchors. Further theoretical, experimental and numerical work is needed to investigate the performance of large single anchors and anchor groups and to improve current design recommendations.

Keywords: anchor bolts, concrete cone failure, edge failure, size effect, finite elements, microplane.

1 INTRODUCTION

In engineering practice headed anchors are often used to transfer loads into reinforced concrete. Experience, as well as a large number of experiments and numerical studies with anchors of different sizes, confirm that fastenings are capable of transfering a tension forces into a concrete member without the need for reinforcement (Eligehausen & Mallée 2000). Provided that the strength of the anchor steel and the load bearing area of the head are large enough, a headed stud subjected to a tensile load normally fails by a cone shaped concrete breakout.

To better understand the crack growth and to predict the concrete cone failure load of headed studs for different embedment depths, a number of experimental and theoretical studies have been carried out (Eligehausen & Mallée 2000). Due to the fact that the tests with large embedment depths require massive test equipment, most of the experiments were performed with embedment depths in the range from $h_{ef} = 100$ to 500 mm. Furthermore, in the tests the size of the headed studs is usually chosen such that the compressive stress under the head at peak load is approximately 15 times larger than the uniaxial compressive strength of concrete. In engineering practice, especially in nuclear power plants, anchors with larger embedment depths and with larger head sizes relative to the embedment depth are frequently used. These anchors are designed according to the current design code recommendations, which are based on the experimental results obtained for fasteners with relatively small embedment depths and head sizes. Therefore, to investigate the safety of these anchors, additional experiments are needed. Since these experiments are extremely expensive, failure capacity of large anchors can alternatively be obtained by numerical analysis.

In the last two decades significant work has been done in the development and further improvement of numerical tools. These tools can be employed in the analysis of non-standard anchorages. Unfortunately, the objectivity of the numerical simulation depends strongly on the choice of the material model. Therefore, the numerical results should be confirmed by experiments and the numerical model used should pass some basic benchmark tests. In the present paper the three-dimensional finite element analysis is carried out using the finite element (FE) code MASA. The code is based on the microplane model for concrete. On a very large number of numerical examples that have been carried out in the past, it has been demonstrated that the code is able to predict failure of concrete and reinforced concrete structures realistically (Ožbolt 2001).

In the first part of the present study concrete cone failure is investigated. The embedment depth is varied from 150 mm up to 1500 mm. Moreover, the influence of the size of the head is also studied. For each embedment depth three different head sizes (small, medium and large) are investigated. In the second part of the paper the behaviour of large headed stud anchors located close to an edge and loaded in shear are investigated. The numerical results are compared with the currently available test data.

2 FINITE ELEMENT CODE

The FE code employed in the present study is mainly aimed to be used for the two- and three-dimensional non-linear analysis of structures made of quasi-brittle materials such as concrete. It is based on the microplane material model (Ožbolt et al. 2001) and a smeared crack approach. To avoid mesh dependent sensitivity, either the crack band approach (Bažant & Oh, 1983) or the nonlocal integral approach (Ožbolt & Bažant 1996, Pijaudier-Cabot & Bažant 1987) can be employed. The spatial discretization of concrete is performed using four or eight node solid finite elements. The reinforcement can be modeled by discrete bar elements with or without discrete bond elements or, alternatively, smeared within the concrete elements. The analysis is carried out incrementally, i.e. the load or displacement is applied in several steps. The preparation of the input data (pre-processing) and evaluation of the numerical results (post-processing) are performed using the commercial program FEMAP®.

In the microplane model, the material properties are characterized on planes of various orientations at a finite element integration point. On these microplanes there are only a few uniaxial stress and strain components and no tensorial invariance requirements need to be considered. The tensorial invariance restrictions are satisfied automatically since the microplanes simulate the response on various weak planes in the material (inter-particle contact planes, interfaces, planes of microcracks, etc.). The constitutive properties are entirely characterized by relations between the normal and shear stress and strain components on each microplane. It is assumed that the strain components on the microplanes are projections of the macroscopic strain tensor (kinematic constraint approach). Knowing the stress-strain relationship of all microplane components, the macroscopic stiffness and the stress tensor are calculated from the actual strains on the microplanes by integrating the stress components on the microplanes over all directions. The simplicity of the model lies in the fact that only uniaxial stress-strain relationships are required for each microplane component and the macroscopic response is obtained automatically by integration over the microplanes. More detail about the model can be found in Ožbolt et al. (2001).

Due to the loss of elipticity of the governing differential equations, the classical local smeared fracture analysis of materials, which exhibit softening (quasi-brittle materials), leads in the finite element analysis to results that are in general mesh dependent. To assure mesh independent results the total energy consumption capacity due to cracking must be independent of the element size, i.e. one has to regularize the problem by introducing a so-called localization limiter. In the present numerical studies the crack band approach (Bažant & Oh 1983) is used. In this approach the constitutive law is related to the element size such that the specific energy consumption capacity of concrete (concrete fracture energy G_F) is independent of the size of the finite element.

3 NUMERICAL ANALYSIS

3.1 *Concrete cone failure of headed studs*

The main purpose of the three-dimensional FE analysis is to investigate how save are anchors with extremely large embedment depths that are pulled-out from a concrete block. The geometry of the concrete block and the geometry of the headed stud are shown in Figure 1. The embedment depth is varied from $h_{ef} = 150$ to 1500 mm. For each embedment depth three head sizes are used (small, medium and large). The geometrical properties for all investigated cases are summarised in Table 1.

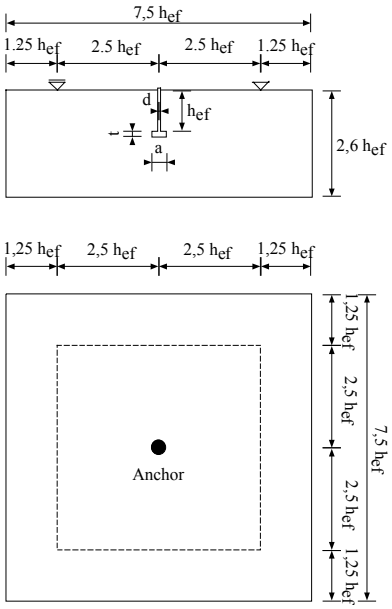

Figure 1. Geometry used in the pull-out study.

Table 1. Geometric properties.

h_{ef} [mm]	d	t	a_1	a_2	a_3
150	16	17	22	31	40
300	33	35.6	41	57	72
635	70	76	83	118	152
889	95.3	102	105	162	216
1500	160.8	169	171	241	311

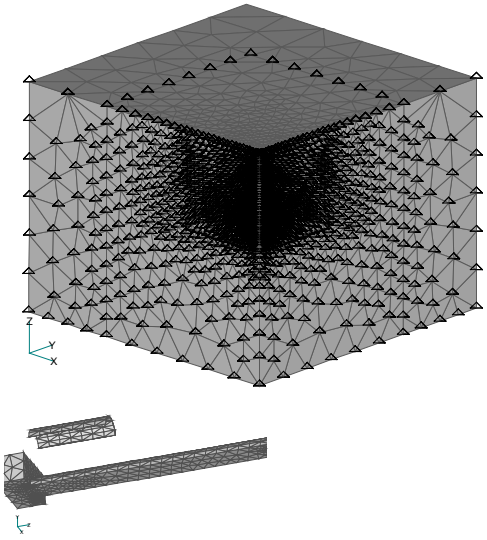

Figure 2. Typical FE meshes of the concrete block and the headed stud with contact elements.

The size of the smallest head for all embedment depths is chosen such that the compressive stress under the head at peak load is 15 times larger than the uniaxial compressive strength of concrete. The peak load is calculated based on the pull-out capacity that is predicted by the CC-design method (Eligehausen & Mallée 2000). The sizes of medium and large anchor heads are taken 1.40 and 1.80 times larger than the small head, respectively. These sizes are chosen to be typical for engineering practice (nuclear power plants). The concrete properties are taken as: Young's modulus $E_C = 28000$ MPa, Poisson's ratio $\nu_C = 0.18$, tensile strength $f_t = 3.0$ MPa, uniaxial compressive strength $f_c = 38$ MPa and concrete fracture energy $G_F = 0.10$ N/mm. The behaviour of steel is assumed to be linear elastic with Young's modulus $E_S = 200000$ MPa and Poisson's ratio $\nu_S = 0.33$.

Spatial discretization is performed using four node solid finite elements. Only one quarter of the concrete block is modelled, i.e. double symmetry is utilized. Typical finite element meshes of the concrete block and headed stud are shown in Figure 2. Contact between the steel stud and concrete exists only on the top of the headed stud (compression transfer zone). To account for the confining stresses that develop in the vicinity of the head, interface elements which can take up only compressive stresses are introduced (see Figure 2). In all cases the anchor is loaded by prescribed displacements at the top of the anchor shaft. The supports were fixed in the vertical (loading) direction. The distance between the support and the anchor is taken as $2.5h_{ef}$ so that an unrestricted formation of the failure cone is possible (see Figure 2).

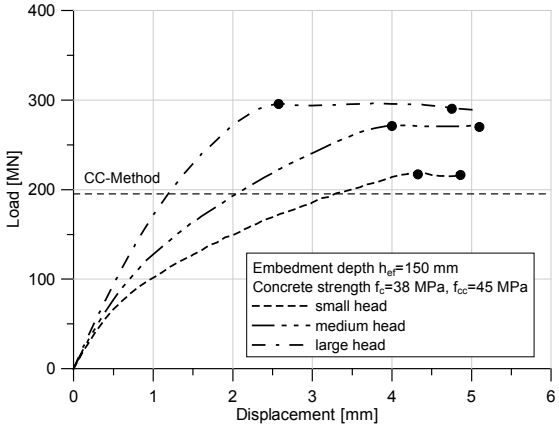

Figure 3. Load-displacement curves for three different head sizes ($h_{ef} = 150$ mm).

Typical load-displacement curves for three different head sizes (h_{ef} = 150 mm) are shown in Figure 3. The curves show that the anchors with small heads have larger displacement at peak load. This tendency is stronger if the embedment depth is larger.

Table 2. Predicted peak loads.

h_{ef} [mm]	Peak load P_U [kN] CC-Method	small head	medium head	large head
150	195.2	219	272	296
300	552	634	824	1044
635	1700	1982	2867	3628
889	2816.7	3313	4635	6048
1500	6173.3	7522	10281	13051

The summary of the predicted peak loads is given in Table 2. In the same table the peak loads obtained according to ETAG CC-design method (Eligehausen & Mallée, 2000):

$$P_U = 15.5\sqrt{f_{cc}}\,h_{ef}^{1.5} \qquad (1)$$

are given as well.

a)

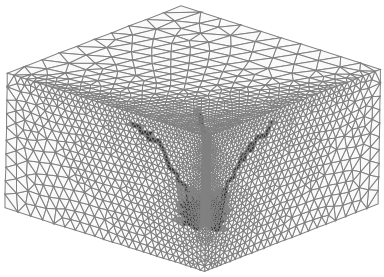

b)

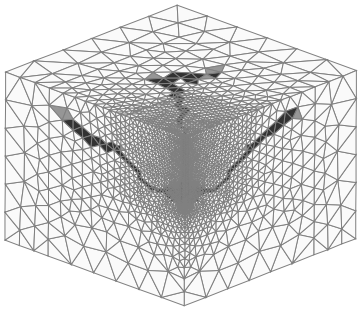

Figure 4. Typical crack patterns: a) small head, h_{ef} = 150 mm and b) large head h_{ef} = 1500 mm.

It should be noted that (1) was calibrated using experiments in which the maximum embedment depth was 500 mm and the head size small, as defined above. Moreover, the exponent 1.5 on the effective depth indicates the size effect on the concrete cone failure resistance according to linear elastic fracture mechanics (LEFM), i.e. maximum possible size effect.

The numerically obtained peak load for h_{ef} = 150 mm and small head size show the best agreement with (1) (a difference of 12%). For large embedment depths the calculated peak load increases relative to (1) and it is largest for h_{ef} = 1500 mm (22%). Keeping in mind that (1) is calibrated for embedment depths up to 500 mm, the agreement between the numerical results and the predictions according to (1) is relatively good for the entire size range. However, for anchors with larger heads the difference between the numerical calculations and (1) is obvious. The larger the head of the anchor, the higher is the predicted failure load. Moreover, the relative differences increase with increase of the embedment depths. The largest difference (111%) between the prediction according to (1) and numerical prediction is obtained for the largest embedment depth and the largest head size.

The calculated crack patterns for two different embedment depths (h_{ef} = 150 mm – small head and h_{ef} = 1500 mm – large head) are shown in Figure 4. The cracks (dark zones) are by means of maximum principal strains. The critical crack opening w_{cr} = 0.2 mm is assumed. This crack opening corresponds to the plotted critical principal strain of $\varepsilon_{cr} = w_{cr}/h_E$, where h_E = average element size. The crack patterns are shown for the peak and the post-peak anchor resistance. It is generally observed that for smaller embedment depths and smaller anchor heads the crack length at peak load is shorter. Moreover, the crack propagation angle measured from the loading direction, increases with increase of both, the embedment depth and the head size. For smaller embedment depths and small head sizes, the concrete cone is much steeper than in the case of large embedment depths and larger head sizes.

The numerical results confirm that there is a strong size effect on the concrete cone failure resistance. In Figure 5 the calculated relative failure resistance ($\sigma_R = \sigma_N/\sigma_{N,hef=150}$, with $\sigma_N = P_U/(h_{ef}^2\pi)$) is plotted as a function of the embedment depth. For comparison the prediction according to (1) is also plotted. Note that the size effect is strong if the gradient of the relative resistance with respect to the embedment depth ($\partial\sigma_R/\partial h_{ef}$) is large. As mentioned above, (1) predicts the maximum size effect (LEFM). From Figure 5 it can be seen that the numerical results for small anchor heads agrees well with (1), i.e. they predict strong size effect. However, with

increase of the relative anchor head size the size effect on the relative anchor resistance decreases. The reason why for fasteners with small anchor head size the size effect agrees well with the size effect prediction according to LEFM is due to the fact that for all embedment depths the crack patterns at peak load are similar - the crack length is relatively small and approximately proportional to the embedment depth. The main assumption of LEFM, namely the proportionality of the crack length at peak load, is fulfilled and therefore size effect is maximal. On the contrary, for fasteners with larger heads the crack pattern for different embedment depths is not proportional. This is the case for both the crack length at peak load, as well as for the shape of the failure cone. Consequently, the size effect on the concrete cone failure load is smaller.

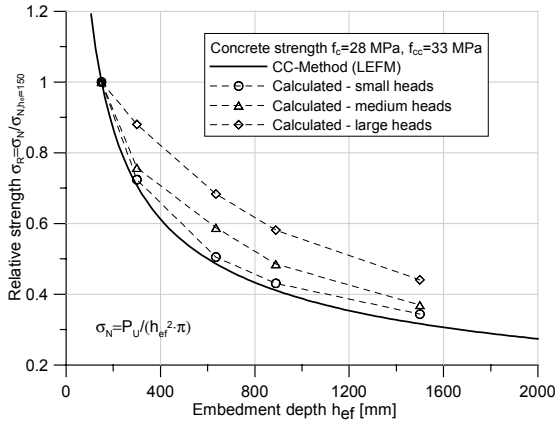

Figure 5. Relative concrete cone resistance as a function of the embedment depth.

In Figure 6 the calculated peak loads are plotted versus the embedment depth. In the same figure the available test data, the prediction according to (1) and the prediction according to ACI 349-01 design formula, that is based on the CC-method for determining anchor resistance, are shown as well. For comparison, the curve which is obtained using the old ACI 349-85 design formula that does not account for the size effect is also shown. All values are plotted assuming a concrete cube strength f_{cc} = 33 MPa (all the data are scaled by the factor $\psi = (33/f_{cc})^{1/2}$). As can be seen from Figure 6, the calculated failure loads for anchors with medium and large heads overestimate predictions obtained from the design code formulas that are based on the CC-method. Therefore, independent of the head size, the anchors with large embedment depths designed according to the current design recommendations are conservative. However, the old ACI 349-85 design formula for larger embedment depths agrees relatively well with the numerical predictions only for very large anchor heads, otherwise, the formula is unconservative.

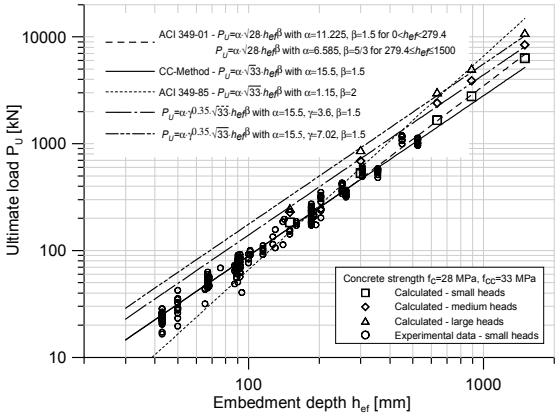

Figure 6. Ultimate load versus embedment depth.

To account for the size effect and to take the influence of the head size into account, based on the numerical results the design formula (1) is extended as:

$$P_U = 15.5\ \gamma^{0.35}\sqrt{f_{cc}}\,h_{ef}^{1.5}$$
$$\gamma = \frac{A}{A_0};\quad A_0 = \frac{P_U}{15 f_c} = \frac{15.5\sqrt{f_{cc}}\,h_{ef}^{1.5}}{15 f_c} \qquad (2)$$

where A = bearing area under the head of the anchor and A_0 = bearing area under the head of the anchor calculated such that for P_U from (1) the ratio $(P_U/A_0)/f_c = 15$). In (2) the assumption is that (1) is valid for anchors which have the bearing area of A_0. The numerical results confirm this assumption for the complete size range investigated. To check the validity of (2) the numerical results are compared in Figure 6 with (2). For small head sizes, the prediction according to (2) coincides with (1). Since for anchors with medium and large head sizes the ratio γ is not the same for all embedment depths, the prediction according to (2) is calculated assuming an average value of γ (medium size heads γ= 3.60 and large heads γ= 7.02). As can be seen from Figure 6, the fit of the calculated data with (2) is good.

In the framework of the experimental investigations on large anchors that are going to be used in the nuclear power plants in Korea, concrete specimens for testing large anchors (h_{ef} = 889 mm, γ= 10.15) were designed. The aim was to check concrete cone failure load. The concrete blocks with dimensions length-width-height of 4760-

2560-1840 mm (KEPRI & KOPEC 2003) were simply supported beams with the support distance of $5h_{ef}$. The material properties were the same as above except: $f_t = 1.0$ MPa, $f_c = 37$ MPa and $G_F = 0.07$ N/mm. Note that f_t and G_F were reduced due to the influence of the damage caused by shrinkage of concrete block. The edge of the specimen was at the distance of approximately $c = 2h_{ef}$ from the anchor. The specimens were designed such that the concrete cone failure takes place under the assumption that (1) is valid. Unfortunately, in the test the concrete specimen failed due to bending (splitting) and not by concrete cone failure. Obviously, the design concrete cone failure load underestimated the real failure capacity of the tested specimen.

The specimen is analysed once with the original geometry and once with doubled specimen height. The peak loads are summarized in Table 3 and the failure modes are shown in Figure 7.

Table 3. Predicted and measured peak loads.

h_{ef} [mm]	Peak load P_U [kN] Test	Eq. (1)	Eq. (2)	Analysis test thickness	Analysis 2 x test thickness
889	2440	2324	5230	2499	2802

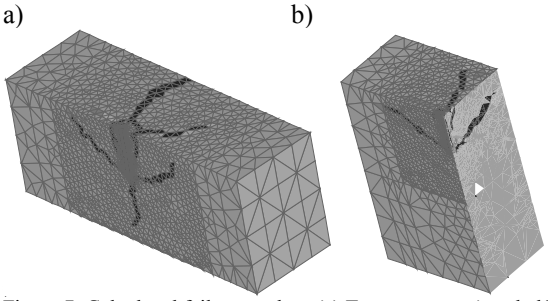

Figure 7. Calculated failure modes : (a) Test geometry (one half of the specimen) and (b) Double specimen thickness – section cut.

The test results and the numerical results for the original geometry agree well. The specimen failed by splitting in both cases (see Fig. 7a). The calculated peak load agrees well with the test results and it is larger than predicted by (1). The analysis of the deeper specimen shows a concrete cone failure (see Fig. 7b). The peak load increases, however, the failure mode indicates a rather strong influence of the edge, i.e. the concrete cone failure surface propagates almost perpendicular to the free surface of the specimen (see Fig. 7b). For the present case the edge distance was $c = 2h_{ef}$, which is for anchors with large heads obviously not enough to obtained an unrestricted concrete cone failure. As the above parameter study shows, for a geometry with no edge influence, (2) should be a more appropriate formula for the design of anchors with larger heads. Obviously, the above experiment is not sufficient to confirm the results of the numerical studies. Therefore, there is a need for further experimental and theoretical studies.

3.2 *Shear failure*

Another aim of the present study was to investigate the behavior of large headed stud anchors loaded in shear. The numerical results are compared with current design recommendations and recent experimental results. It should be noted that the numerical study was performed before the test data were available.

The geometry used in the present study is shown in Figure 8. The geometrical data for all five different geometries are summarized in Table 4.

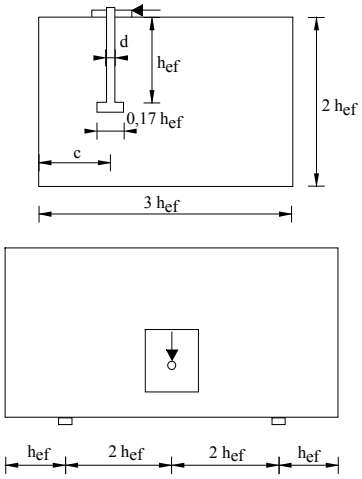

Figure 8. Geometry used in the shear finite element study.

Table 4. Geometrical properties

Specimen	Anchor Diameter d [mm]	Embedment Depth h_{ef} [mm]	Edge Distance c [mm]
S1	63.5	635	508
S2	76.2	635	508
S3	88.9	635	508
S4	76.2	889	508
S5	63.5	635	229

The analysis is performed for two different embedment depths ($h_{ef} = 635$ and 889 mm), for two different edge distances ($c = 229$ and 508 mm) and for three different anchor diameters ($d = 63.5$, 76.2 and 88.9 mm). The concrete properties are taken as: Young's modulus $E_C = 30000$ MPa, Poisson's ratio $\nu_C = 0.18$, tensile strength $f_t = 2.7$ MPa, uniaxial compressive strength $f_c = 38.0$ MPa,

concrete fracture energy $G_F = 0.1$ N/mm and concrete compressive fracture energy $G_C = 100 G_F$. These concrete properties were design properties for the experiments. In subsequently performed experiments these values were only approximately reached, i.e. the average uniaxial compressive strength of concrete in the test was 37.6 MPa. All other properties are not known. The behavior of steel (anchors and anchor plate) is assumed to be linear elastic with Young's modulus $E_S = 200000$ MPa and Poisson's ratio: $\nu_S = 0.33$. The contact between concrete and steel and contact between the anchor plate and the concrete is modelled by an interface element which can transfer only compressive stresses. The typical finite element mesh is shown in Figure 9. Table 5 summarizes the numerical results and the available experimental results.

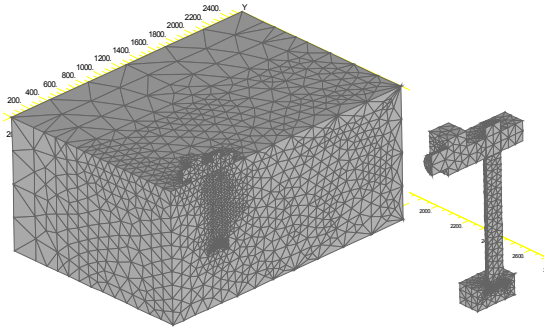

Figure 9. Finite element discretization – concrete block and anchor bolt (symmetry - 1/2 of the geometry).

Table 5. Calculated results – peak loads in [kN]

Specimen	Calculated	Test	Equation (4)	Equation (3)
S1	608	496	513	835
S2	594	470	531	915
S3	591	494	554	966
S4	607	NA	594	915
S5	175	NA	210	253

In the experiments the diameter of the bolt was varied whereas all other parameters were kept constant. The calculated and measured peak loads for three different diameters of the bolt are shown in Figure 10. Keeping in mind that the numerical analysis was carried out before the test results were known and due to the fact that the concrete properties in the experiments were most probably not identical to those used in the analysis, the agreement between absolute values of predicted and measured peak loads is good. More importantly, the analysis and the experiments show that for investigated anchors the bolt diameter has no influence on the resistance. For comparison, in the same figure the predictions according to the currentl design formula:

$$V_U = 0.9\sqrt{d}\left(\frac{h_{ef}}{d}\right)^{0.2}\sqrt{f_{cc}}\,c^{1.5};\quad h_{ef} \le 8d \tag{3}$$

and according to the recently proposed formula (Hofmman, 2003):

$$V_U = 3 d^{\alpha} h_{ef}^{\beta}\sqrt{f_{cc}}\,c^{1.5}$$
$$\alpha = 0.1\left(h_{ef}/c\right)^{0.5};\quad \beta = 0.1\left(d/c\right)^{0.2} \tag{4}$$

are shown as well. As can be seen, the design formula (3) overestimates the test and calculated peak loads by almost a factor of two and, in contrast to the test and numerical data, indicates an increase of the peak resistance with increasing bolt diameter. The recently proposed formula (4), however, shows good agreement with the test and the calculated data.

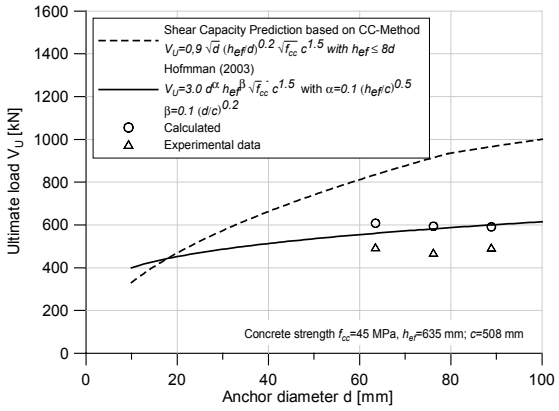

Figure 10. Calculated peak loads versus anchor diameter.

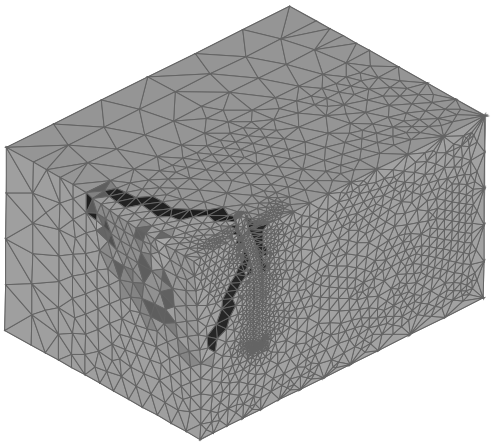

Figure 11. Typical crack pattern obtained from the analysis.

The typical crack pattern obtained from the analysis is shown in Figure 11. It is almost identical to that obtained in the experiment (KEPRI & KOPEC, 2003). The crack propagates under an average angle of 35 degrees, measured parallel to the edge of the specimen. In Figs. 12 and 13 the calculated failure loads are plotted as a function of the edge distance and embedment depth, respectively. For plotted values all other geometrical parameters were kept constant. For comparison, the available test data and predictions according to (3) and (4) are shown as well. Similar as for the influence of the bolt diameter, the current design formula significantly overestimates the peak resistance obtained numerically. On the contrary, the numerical results, the test results and the recently proposed formula (4) show good agreement.

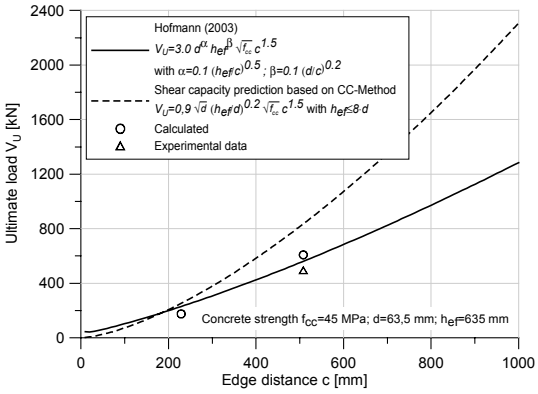

Figure 12. Calculated peak loads versus edge distance.

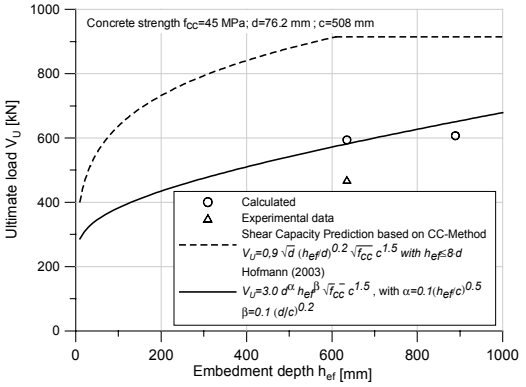

Figure 13. Calculated peak loads versus embedment depth.

4 CONCLUSIONS

In the present study the behavior of large anchor bolts embedded in concrete is numerically investigated. Two load cases are studied: (i) pull-out from a concrete block (concrete cone failure) and (ii) shear load against a concrete edge (concrete edge failure). The numerical results are compared with available test data and current design recommendations. Based on the results, the following can be concluded: (1) Calculated concrete cone capacity for large anchors and small heads shows good agreement with current design formula that is based on LEFM. The analysis also confirms the strong size effect on the concrete cone resistance. By increasing the size of the headed stud the peak load increases and the size effect decreases. To account for the effect of the head size an additional influencing factor is proposed. Although there are limited experimental results available for larger anchors, the performed experiments indirectly confirm numerical results; (2) Numerical results for large anchors obtained for concrete edge failure agree well with the test results. Both indicate that the currently valid design formula is unsafe for large anchor. A more recently proposed formula fits much better to the experimental and numerical results; (3) To improve and extend the validity of current design recommendations further theoretical, experimental and numerical work is needed.

5 REFERENCES

ACI Standard 349-85. 1985. *Code Requirements for Nuclear Safety Related Concrete Structures*, Appendix B - Steel Embedments.

ACI Standard 349-01/349R-01. 2001. *Code Requirements for Nuclear Safety Related Concrete Structures and Commentary (ACI 349R-01)*.

Bažant, Z.P. and Oh, B.-H. 1983. Crack Band Theory for Fracture of Concrete. *Materials and Structures*, *RILEM*, 93(16): 155-177.

Eligehausen, R. and Mallée, R. 2000. *Befestigungstechnik im Beton- und Mauerwerkbau*, Ernst & Sohn, Berlin, Germany.

Hofmman, J. 2003. *Headed Studs Anchros Under Shear Load*, PhD. Thesis in preparation, University of Stuttgart, Stuttgat, Germany.

KEPRI & KOPEC. 2003. Internal Report on: *Pre-tests for Large-sized Cast-in-place Anchors*. Korea.

Ožbolt, J. and Bažant, Z.P. 1996. Numerical smeared fracture analysis: Nonlocal microcrack interaction approach. *International Journal for Numerical Methods in Engineering*, 39(4): 635-661.

Ožbolt, J., Li, Y.-J. and Kožar, I. 2001. Microplane model for concrete with relaxed kinematic constraint. *International Journal of Solids and Structures*. 38: 2683-2711.

Ožbolt, J. 2001. Smeared fracture finite element analysis – Theory and examples. R. Eligehausen (ed), *International symposium on Connections between Steel and Concrete*: 609-624. RILEM Publication, SARL.

Pijaudier-Cabot, G. and Bažant, Z.P. 1987. Nonlocal Damage Theory. *Journal of Engineering Mechanics*, *ASCE*, 113(10): 1512-1533.